

# Implicit self-consistent description of electrolyte in plane-wave density-functional theory

Kiran Mathew<sup>1,2,\*</sup> and Richard G. Hennig<sup>2,†</sup>

<sup>1</sup>*Department of Materials Science, Cornell University, Ithaca, New York 14853, USA*

<sup>2</sup>*Department of Materials Science, University of Florida, Gainesville, Florida 32608, USA*

(Dated: July 15, 2018)

Ab-initio computational treatment of electrochemical systems requires an appropriate treatment of the solid/liquid interfaces. A fully quantum mechanical treatment of the interface is computationally unfeasible due to the large number of degrees of freedom involved. In this work we describe a computationally efficient model where the electrode part of the interface is modeled at the density functional theory (DFT) level and the electrolyte part is represented through an implicit model based on the Poisson-Boltzmann equation. We describe the implementation of the model Vienna Ab-initio Simulation Package (VASP), a widely used DFT code, followed by validation and benchmarking of the implementation. To demonstrate the utility of the implicit electrolyte model we apply the model to study the effect of electrolyte and external voltage on the surface diffusion of sodium atoms on the electrode.

PACS numbers:

## I. INTRODUCTION

Interfaces between dissimilar systems are ubiquitous in nature and frequently encountered and employed in scientific and engineering applications. Of particular interest are solid/liquid interfaces that form the crux of many technologically important systems such as electrochemical interfaces,<sup>1–3</sup> nanoparticle synthesis,<sup>4–6</sup> and protein folding and membrane formation.<sup>7</sup> A comprehensive understanding of the behavior and properties of such systems requires a detailed microscopic description of the solid/liquid interfaces.

Given the heterogeneous nature and the complexities of solid/liquid interfaces,<sup>8</sup> it is often the case that experimental studies need to be supplemented by theoretical undertakings. A complete theoretical study of such interface based on an explicit description of the electrolyte and solute involves solving systems of nonlinear equations with enormous amount of degrees of freedom and quickly become prohibitively expensive even when state of the art computational resources are employed.<sup>9</sup> This calls for the development of efficient implicit computational frameworks for the study of solid/liquid interfaces.<sup>9–14</sup>

We have previously developed a self-consistent solvation model<sup>15,16</sup> that describes the dielectric screening of a solute embedded in an implicit solvation model for the solvent, where the solute is described by density-functional theory (DFT). We implemented this solvation model into the widely used DFT code VASP.<sup>17</sup> This software package, VASPsol, is freely available under the GPL v3 license and has been used by us and others to study the effect of the presence of solvent on a number of materials and processes, such as the catalysis of ketone hydrogenation,<sup>18</sup> the interfacial chemistry in electrochemical interfaces,<sup>19</sup> hydrogen adsorption on platinum surfaces,<sup>20</sup> *etc.*

In this work we describe the extension of our solvation model VASPsol<sup>15,16</sup> to include the effects of mobile ions

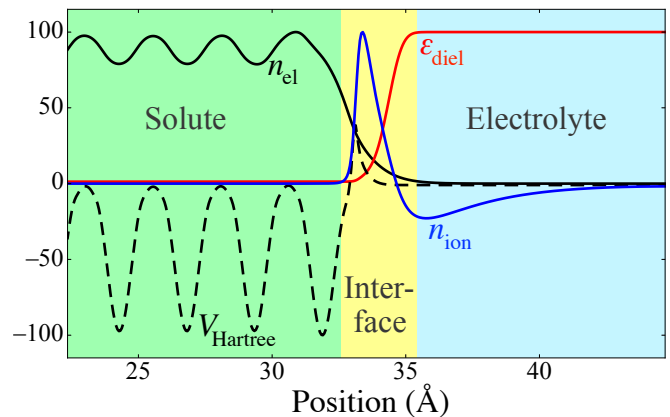


FIG. 1: Spatial decomposition of the solid/electrolyte system into the solute, interface, and electrolyte regions for a bcc Na(110) surface embedded in an electrolyte with relative permittivity  $\epsilon_r = 78.4$  and monovalent cations and anions with concentration 1M. The solute is described by density-functional theory, the electrolyte by an implicit solvation model. The interface regions is formed self-consistently as a functional of the electronic density of the solute. All properties are shown as a percentage of their maximum absolute value.

in the solvent through the solution of the linear Poisson-Boltzmann equation and then apply the method to electrochemical systems to illustrate the power of this approach. Figure 1 illustrates how the solid/electrolyte system is divided into spatial regions that are described by the explicit DFT and the implicit solvation model. This new solvation model allows for the description of charged systems and the study of the electrochemical interfacial systems under applied external voltage. Section II describes the formalism and outlines the derivation of the energy expression. In Sec. III we describe the details of the implementation and validate the method against pre-

vious computational studies of electrochemical systems. Finally, in Sec. IV we apply the method to study the effect of an applied external potential on the adsorption and surface diffusion for metal electrodes.

## II. THEORETICAL FRAMEWORK

Our solvation model couples an implicit description of the electrolyte to a quantum-mechanical explicit description of the solute. The implicit solvation model incorporates the dielectric screening due to the permittivity of the solvent and the electrostatic shielding due to the mobile ions in the electrolyte. The solute is described explicitly using DFT.

To obtain the energy of the combined solute/electrolyte system, we spatially divide the materials system into three regions: (i) the solute that we describe explicitly using DFT, (ii) the electrolyte that we describe using the linear Poisson-Boltzmann equation and (iii) the interface region, that electrostatically couples the DFT and Poisson-Boltzmann equation. Fig. 1 illustrates the regions for a Na(110) surface embedded in a 1M aqueous electrolyte. The interface between the electrolyte and the solute system is formed self-consistently through the electronic density and the interaction between the electrolyte and solute is described by the electrostatic potential as explained in the following sections.

### A. Total energy

We define the interface region between the solute and the electrolyte using the electronic charge density of the solute,  $n(\vec{r})$ . The electrolyte occupies the volume of the simulation cell where the solute charge density goes to zero. In the interface region where the electronic charge density increases rapidly from zero towards the average bulk value of the solute, the properties of the implicit solvation model, *e.g.* the permittivity  $\epsilon$  and the Debye screening length  $\lambda_D$ , change from their bulk values of the electrolyte to the vacuum values in the explicit region. The scaling of the electrolyte properties is given by a shape function<sup>11,15,21–23</sup>

$$S(n(\vec{r})) = \frac{1}{2} \operatorname{erfc} \left\{ \frac{\log(n/n_c)}{\sigma\sqrt{2}} \right\}. \quad (1)$$

Following our previous work<sup>15</sup> and the work by Arias *et al.*,<sup>11,21–23</sup> the total free energy,  $A$ , of the system consisting of the solute and electrolyte is expressed as

$$\begin{aligned} A[n(\vec{r}), \phi(\vec{r})] &= A_{\text{TXC}}[n(\vec{r})] + \int \phi(\vec{r}) \rho_s(\vec{r}) d^3r \\ &\quad - \int \epsilon(\vec{r}) \frac{|\nabla\phi|^2}{8\pi} d^3r + \int \frac{1}{2} \phi(\vec{r}) \rho_{\text{ion}}(\vec{r}) d^3r \\ &\quad + A_{\text{cav}} + A_{\text{ion}}, \end{aligned} \quad (2)$$

where  $A_{\text{TXC}}$  is the kinetic and exchange-correlation contribution from DFT,  $\phi$  is the net electrostatic potential of the system, and  $\rho_s$  and  $\rho_{\text{ion}}$  are the total charge density of the solute and the ionic charge density of the electrolyte, respectively. The net solute charge density,  $\rho_s$ , is the sum of the solute electronic and nuclear charge densities,  $n(\vec{r})$  and  $N(\vec{r})$ , respectively,

$$\rho_s(\vec{r}) = n(\vec{r}) + N(\vec{r}). \quad (3)$$

The net ionic charge density,  $\rho_{\text{ion}}$ , is given by

$$\rho_{\text{ion}}(\vec{r}) = \sum_i q z_i c_i(\vec{r}), \quad (4)$$

where  $c_i(\vec{r})$  is the concentration of ionic species  $i$  with charge  $z_i q$ , and  $q$  is the elementary charge. The concentration of ionic species,  $c_i$ , is given by a Boltzmann factor of the electrostatic energy<sup>24</sup> and modulated in the interface region by the shape function,  $S(n(\vec{r}))$ ,

$$c_i(\vec{r}) = S[n(\vec{r})] c_i^0 \exp \left( \frac{-z_i q \phi(\vec{r})}{kT} \right), \quad (5)$$

where  $c_i^0$  is the bulk concentration of ionic species  $i$ ,  $k$  is the Boltzmann constant and  $T$  the temperature. The relative permittivity of the electrolyte,  $\epsilon(\vec{r})$ , is assumed to be a local functional of the electronic charge density of the solute and modulated by the shape function,<sup>11,15,21–23</sup>

$$\epsilon(n(\vec{r})) = 1 + (\epsilon_b - 1) S(n(\vec{r})), \quad (6)$$

where  $\epsilon_b$  is the bulk relative permittivity of the solvent. The cavitation energy,  $A_{\text{cav}}$ , describes the energy required to form the solute cavity inside the electrolyte and is given by<sup>14</sup>

$$A_{\text{cav}} = \tau \int |\nabla S| d^3r. \quad (7)$$

In comparison to our previous solvation model,<sup>15</sup> the main changes to the free energy expression are the inclusion of the electrostatic interaction of the ionic charge density in the electrolyte with the system's electrostatic potential,  $\phi$ , and the non-electrostatic contribution to the free energy from the mobile ions in the electrolyte,  $A_{\text{ion}}$ . In this work we assume that to be just the entropic contribution,<sup>24</sup> *i.e.*

$$A_{\text{ion}} = kT S_{\text{ion}}, \quad (8)$$

where  $S_{\text{ion}}$  is the entropy of mixing of the ions in the electrolyte, which for small electrostatic potentials can be approximated to first order as

$$\begin{aligned} S_{\text{ion}} &= \int \sum_i c_i \ln \left( \frac{c_i}{c_i^0} \right) d^3r \\ &\approx - \int \sum_i c_i \frac{z_i q \phi}{kT} d^3r. \end{aligned} \quad (9)$$

## B. Minimization

To obtain the stationary point of the free energy,  $A$ , given by Eq. (2), we set the first order variations of the free energy with respect to the system potential,  $\phi$ , and the electronic charge density,  $n(r)$ , to zero.<sup>11,15,21–23</sup> Taking the variation of  $A[n(\vec{r}), \phi(\vec{r})]$  with respect to the electronic charge density,  $n(\vec{r})$ , yields the typical Kohn-Sham Hamiltonian<sup>25</sup> with the following additional term in the local part of the potential

$$V_{\text{solv}} = \frac{\delta\epsilon(n)}{\delta n} \frac{|\nabla\phi|^2}{8\pi} + \phi \frac{\delta\rho_{\text{ion}}}{\delta n} + \tau \frac{\delta|\nabla S|}{\delta n} + kT \frac{\delta S_{\text{ion}}}{\delta n}. \quad (10)$$

Taking the variation of  $A[n(\vec{r}), \phi(\vec{r})]$  with respect to  $\phi(\vec{r})$  yields the generalized Poisson-Boltzmann equation

$$\vec{\nabla} \cdot \epsilon \vec{\nabla} \phi = -\rho_s - \rho_{\text{ion}}, \quad (11)$$

where  $\epsilon(n(r))$  is the relative permittivity of the solvent as a functional of the electronic charge density.

We further simplify the system by considering the case of electrolytes with only two types of ions present, whose charges are equal and opposite, *i.e.*  $c_1^0 = c_2^0 = c^0$  and  $z_1 = -z_2 = z$ . Then the ionic charge density of the electrolyte becomes<sup>24</sup>

$$\begin{aligned} \rho_{\text{ion}} &= qzc^0 \left[ \exp\left(\frac{-zq\phi}{kT}\right) - \exp\left(\frac{zq\phi}{kT}\right) \right] \\ &= -2qzc^0 \sinh\left(\frac{zq\phi}{kT}\right) \end{aligned} \quad (12)$$

and the Poisson-Boltzmann equation becomes

$$\vec{\nabla} \cdot \epsilon \vec{\nabla} \phi = -\rho_s + 2qzc^0 \sinh\left(\frac{zq\phi}{kT}\right). \quad (13)$$

For small arguments  $x = \frac{zq\phi}{kT} \ll 1$ ,  $\sinh(x) \rightarrow x$  and we obtain the linearized Poisson-Boltzmann equation

$$\vec{\nabla} \cdot \epsilon \vec{\nabla} \phi - \kappa^2 \phi = -\rho_s \quad (14)$$

with

$$\kappa^2 = \left( \frac{2c^0 z^2 q^2}{kT} \right) = \frac{1}{\lambda_D^2}, \quad (15)$$

where  $\lambda_D$  is the Debye length that characterizes the dimension of the electrochemical double layer.

## III. IMPLEMENTATION AND VALIDATION

The implicit electrolyte model described above is implemented in the widely used DFT software Vienna Ab-initio Software Package (VASP).<sup>17</sup> VASP is a parallel plane-wave DFT code that supports both ultra-soft

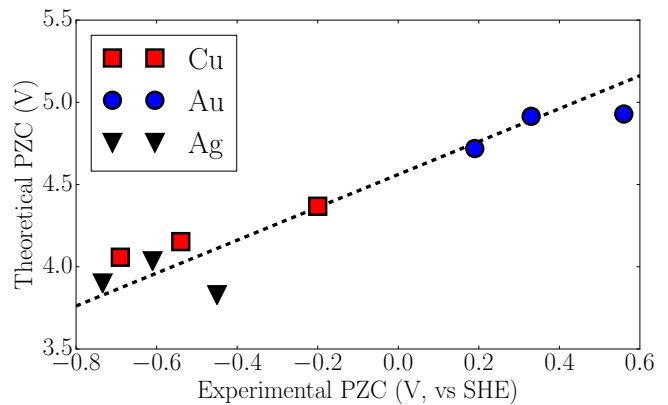


FIG. 2: Comparison between the computed and the experimental Potential of Zero Charge (PZC) with respect to the standard hydrogen electrode (SHE). The dashed line is a fit of  $V^{\text{pred}} = V^{\text{exp}} + V_{\text{SHE}}^{\text{pred}}$  to determine the theoretical potential of the SHE.

pseudopotentials<sup>26,27</sup> as well as the PAW<sup>28</sup> formulation of pseudopotentials.

The main modifications in the code are the evaluation of the additional contributions to the total energy and the local potential given by Eqs. (2) and (10), respectively. Corrections to the local potential require the solution of the generalized Poisson-Boltzmann equation (13) in each self-consistent iteration. Our implementation solves the equation in reciprocal space and makes efficient use of fast Fourier transformations (FFT).<sup>15</sup> This enables our implementation to be compatible with the Message Passing Protocol (MPI) and to take advantage of the memory layout of VASP. We use a preconditioned conjugate gradient algorithm to solve the generalized Poisson-Boltzmann equation with the preconditioner  $(G^2 + \kappa^2)^{-1}$ , where  $G$  is the magnitude of the reciprocal lattice vector and  $\kappa^2$  is the inverse of the square of the Debye length,  $\lambda_D$ . Our software module, VASPsol, is freely distributed as an open-source package and hosted on GitHub at <https://github.com/henniggroup/VASPsol>.<sup>16</sup>

We benchmark the model against existing experimental and computational data.<sup>21</sup> First, we compute the potential of zero charge (PZC) of various metallic slabs and compare them against the experimental values. Second, we compute the surface charge density of a Pt(111) slab as function of the applied external potential and compare the resulting value of the double layer capacitance with previous computation and experiment.

The DFT calculations for these two benchmarks are performed with VASP and the VASPsol module using projected augmented wave (PAW) formalism describing the electron-ion interactions and the PBE approximation for the exchange-correlation functional.<sup>17,29</sup> The Brillouin-zone integration uses an  $8 \times 8 \times 1$   $k$ -points. A high plane-wave basis set cutoff energy of 800 eV is used to ensure proper resolution of the interfacial region be-

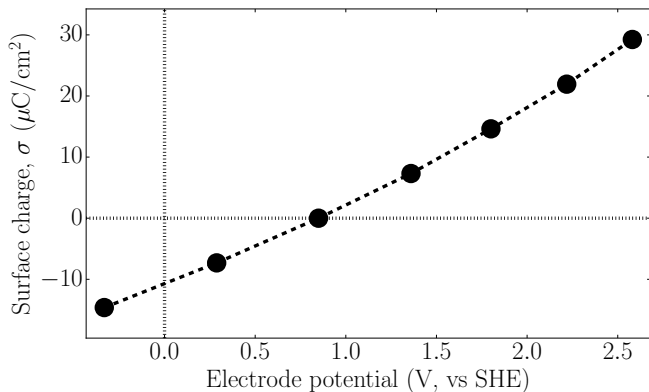


FIG. 3: Surface charge density of the Pt(111) surface as a function of applied electrostatic potential computed with the implicit electrolyte module, VASPsol. The slope of the curve determines the capacitance of the dielectric double layer.

tween the solute and implicit. We consider an electrolyte that consists of an aqueous solution of monovalent anions and cations of 1M concentration. At room temperature this electrolyte has a relative permittivity of  $\epsilon_b = 78.4$  and a Debye length of 3 Å. To change the applied potential, we adjust the electron count and then determine the corresponding potential from the shift in electrostatic potential as reflected in the shift in Fermi level. This takes advantage of the fact that the electrostatic potential goes to zero in the electrolyte region for the solution of the Poisson-Boltzmann equation.

Figure 2 compares the electrode potential of zero charge (PZC) calculated with the implicit electrolyte model as implemented in VASPsol with experimental data. The electrode potential of zero charge is defined as the electrostatic potential of a neutral metal electrode and is given by the Fermi energy with respect to a reference potential. A natural choice of reference for the implicit electrolyte model is the electrostatic potential in the bulk of the electrolyte, which is zero in any solution of the Poisson-Boltzmann equation. In experiments, the reference is frequently chosen as the standard-hydrogen electrode (SHE). The dashed line in Fig. 2 presents the fit of  $V^{\text{pred}} = V^{\text{exp}} + V_{\text{SHE}}^{\text{pred}}$  to obtain shift between the experimental PZC and the computed PZC, . *i.e.* the potential of the SHE for our electrolyte model. The resulting  $V_{\text{SHE}}^{\text{pred}} = 4.6$  V compares very well with the previously reported computed value of 4.7 V for a similar solvation model.<sup>23</sup>

Figure 3 shows the calculated surface charge density,  $\sigma$ , of the Pt(111) surface as a function of applied electrostatic potential,  $V$ . The linear slope of  $\sigma(V)$  is the double-layer capacitance. The resulting double-layer capacitance for the Pt(111) surface at 1M concentration is 15  $\mu\text{F}/\text{cm}^2$ , which closely agrees with the previously reported computed<sup>23</sup> and experimental<sup>30</sup> values of 14  $\mu\text{F}/\text{cm}^2$  and 20  $\mu\text{F}/\text{cm}^2$ , respectively. The discrepancy between the VASPsol value of the double layer

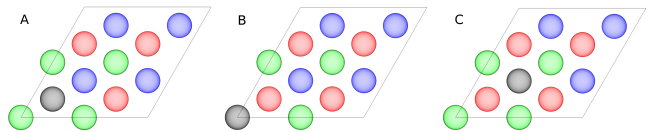


FIG. 4: Pt adatom(black) adsorbed on three different sites on the Pt 111 surface. Red, green and blue indicate top, second and third layers of Pt 111 respectively

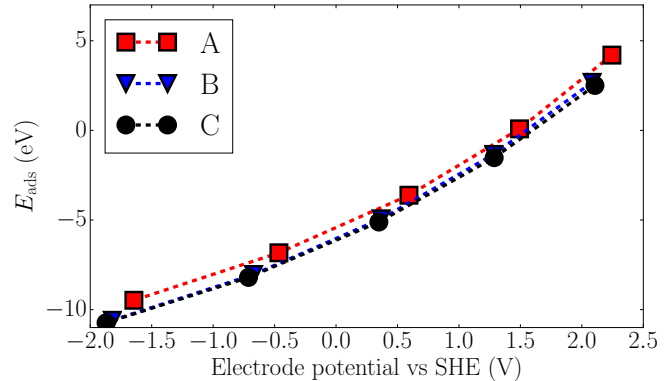


FIG. 5: Plot of voltage vs the adsorption energy

capacitance and the computed value in the literature can be attributed to the difference in pseudo-potentials.

#### IV. APPLICATIONS

The implicit electrolyte model, VASPsol, enables the study the electrode surfaces in realistic environments and under various conditions, such as of an electrode immersed in an electrolyte with an external potential applied. To illustrate the utility of the solvation model, we apply it to study the adsorption energy and diffusion energy barrier of an adatom on a metallic electrode that is immersed in a 1M aqueous electrolyte as a function of applied potential.

Stability of fuel cell materials plays a significant role in the the development of polymer electrolyte fuel cells(PEFCs). PEFC performance loss under steady-state and cycling conditions has been attributed in part to a loss of electrochemically active surface area of the platinum cathode electro-catalyst<sup>31</sup>. In this work we study the dissolution of Pt electrode by looking at the adsorption energies of Pt adatom on Pt 111 surfaces. We apply the implicit electrolyte model to simulate the Pt electrode under external potential. For the adsorption, three adsorption sites are considered, labeled A, B and C, as shown in Figure 4. The plot of adsorption energy as a function of the externally applied potential is shown in the Figure 5. From the plot it can be observed that the adsorption energy increases as the potential is ramped up. This implies that the Pt adatom is less likely to adsorb on to the Pt 111 surface at higher

potentials i.e rate of dissolution is higher at larger potentials. The observation is corroborated by previous experimental studies<sup>31,32</sup>, thus demonstrating the practical applicability of the model.

## V. CONCLUSIONS

Solid/liquid interfaces between electrodes and electrolytes in electrochemical cells present a complex system that requires the insights provided by computational studies to supplement and explain experimental observations. We developed and implemented a self-consistent computational framework that provides an efficient implicit description of electrode/electrolyte interfaces within density-functional theory through the solution of the generalized linear Poisson-Boltzmann equation. The electrolyte model is implemented in the widely used DFT code VASP and the implementation is made available as a free and open-source module, VASPsol. We show that this model enables ab-initio studies of electrochemistry at the DFT level. We validate the model

by comparing the calculated electrode potential of zero charge for various metal electrodes with experimental values and by comparing the calculated double-layer capacitance of Pt(111) in a 1M solution and to previously calculations and experiments. To illustrate the usefulness of the model and the implementation, we compute the adsorption energy of Pt adatoms on a Pt(111) electrode as function of the applied potential. Confirming previous experimental observations, we find that the Pt dissolution rate increases as a function of the externally applied potential.

## Acknowledgments

This work was supported by the National Science Foundation under the CAREER award No. DMR-1056587 and under award No. ACI-1440547. This research used computational resources of the Texas Advanced Computing Center under Contract Number TG-DMR050028N and of the University of Florida Research Computing Center.

- 
- \* Electronic address: km468@cornell.edu  
 † Electronic address: rhennig@mse.ufl.edu
- <sup>1</sup> D. Wang, H. L. Xin, Y. Yu, H. Wang, E. Rus, D. A. Muller, and H. D. Abrua, *J. Am. Chem. Soc.* **132**, 17664 (2010).
  - <sup>2</sup> D.-H. Ha, M. A. Islam, and R. D. Robinson, *Nano Lett.* **12**, 5122 (2012).
  - <sup>3</sup> G. Liu, E. Luais, and J. J. Gooding, *Langmuir* **27**, 4176 (2011).
  - <sup>4</sup> J. J. Choi, C. R. Bealing, K. Bian, K. J. Hughes, W. Zhang, D.-M. Smilgies, R. G. Hennig, J. R. Engstrom, and T. Hanrath, *J. Am. Chem. Soc.* **133**, 3131 (2011).
  - <sup>5</sup> D. F. Moyano and V. M. Rotello, *Langmuir* **27**, 10376 (2011).
  - <sup>6</sup> T.-F. Liu, Y.-P. Chen, A. A. Yakovenko, and H.-C. Zhou, *Journal of the American Chemical Society* **134**, 17358 (2012), pMID: 23043458.
  - <sup>7</sup> K. A. Dill, S. Bromberg, K. Yue, K. M. Fiebig, D. P. Yee, P. D. Thomas, and H. S. Chan, *Protein Science: A Publication of the Protein Society* **4**, 561602 (1995).
  - <sup>8</sup> V. A. Agubra and J. W. Fergus, *Journal of Power Sources* **268**, 153 (2014), ISSN 0378-7753.
  - <sup>9</sup> S. Ismail-Beigi and T. A. Arias, *Comp. Phys. Comm.* **128**, 1 (2000).
  - <sup>10</sup> J. A. White, E. Schwegler, G. Galli, and F. Gygi, *Journal of Chemical Physics* **113** (2000).
  - <sup>11</sup> S. A. Petrosyan, A. A. Rigos, and T. A. Arias, *J. Phys. Chem. B* **109**, 15436 (2005).
  - <sup>12</sup> C. J. Cramer and D. G. Truhlar, *Accounts of Chemical Research* **41**, 760 (2008).
  - <sup>13</sup> J. Lischner and T. A. Arias, *J. Chem. Phys. B* **114**, 1946 (2010).
  - <sup>14</sup> O. Andreussi, I. Dabo, and N. Marzari, *J. Chem. Phys.* **136**, 064102 (2012).
  - <sup>15</sup> K. Mathew, R. Sundararaman, K. Letchworth-Weaver, T. A. Arias, and R. G. Hennig, *The Journal of Chemical Physics* **140**, 084106 (2014).
  - <sup>16</sup> K. Mathew and R. G. Hennig, *VASPsol - Solvation model for the plane wave DFT code VASP*, <https://github.com/henniggroup/VASPsol> (2015).
  - <sup>17</sup> G. Kresse and J. Furthmüller, *Comput. Mater. Sci.* **6**, 15 (1996).
  - <sup>18</sup> C. Michel, J. Zaffran, A. M. Ruppert, J. Matras-Michalska, M. Jedrzejczyk, J. Grams, and P. Sautet, *Chemical Communications* **50**, 12450 (2014).
  - <sup>19</sup> N. Kumar, K. Leung, and D. J. Siegel, *Journal of The Electrochemical Society* **161**, E3059 (2014).
  - <sup>20</sup> S. Sakong, M. Naderian, K. Mathew, R. G. Hennig, and A. Groß, *The Journal of chemical physics* **142**, 234107 (2015).
  - <sup>21</sup> K. Letchworth-Weaver and T. A. Arias, *Phys. Rev. B* **86**, 075140 (2012).
  - <sup>22</sup> R. Sundararaman, D. Gunceler, K. Letchworth-Weaver, and T. A. Arias. (2012), *JDFTx*. <http://jdfdx.sourceforge.net>.
  - <sup>23</sup> D. Gunceler, K. Letchworth-Weaver, R. Sundararaman, K. A. Schwarz, and T. A. Arias, *Modelling Simul. Mater. Sci. Eng.* **21**, 074005 (2013).
  - <sup>24</sup> K. A. Sharp and B. Honig, pp. 7684–7692 (1990).
  - <sup>25</sup> W. Kohn and L. J. Sham, *Phys. Rev.* **140**, A1133 (1965).
  - <sup>26</sup> D. Vanderbilt, *Phys. Rev. B* **41**, 7892 (1990).
  - <sup>27</sup> G. Kresse and D. Joubert, *Phys. Rev. B* **59**, 1758 (1999).
  - <sup>28</sup> P. E. Blöchl, *Phys. Rev. B* **50**, 17953 (1994).
  - <sup>29</sup> J. P. Perdew, K. Burke, and M. Ernzerhof, *Phys. Rev. Lett.* **77**, 3865 (1996).
  - <sup>30</sup> A. Tymosiak-Zieliska and Z. Borkowska, *Electrochimica Acta* **46**, 3063 (2001), ISSN 00134686.
  - <sup>31</sup> X. Wang, R. Kumar, and D. J. Myers, *Electrochemical and Solid-State Letters* **9**, A225 (2006), ISSN 10990062.
  - <sup>32</sup> P. J. Ferreira, G. J. la O, Y. Shao-Horn, D. Morgan, R. Makharia, S. Kocha, and H. A. Gasteiger, *Journal*

